The influence of sea level rise and changes in fringing reef morphology on gradients in alongshore sediment transport

A. E. Grady,[1] L. J. Moore,[2] C. D. Storlazzi,[3] E. Elias,[4] and M. A. Reidenbach[1]

[1] Climate-change-induced alterations to coral reef ecosystems, in combination with sea level rise, have the potential to significantly alter wave dissipation across reefs, leading to shifts in alongshore sediment transport gradients and alterations to tropical coastlines. We used Delft3D to model schematized profiles of two reef flat widths based on the south Molokai, Hawaii coast. Simulated anthropogenic modifications include incremental degradation of the reef structure as well as sea level rise. Our findings indicate that sea level rise has a greater relative effect on wave energy flux and alongshore sediment transport over a wide flat, whereas both reef degradation and sea level rise exert similar influence over a narrow flat. These results suggest reefs that vary in width alongshore are more likely to experience changes in alongshore sediment transport gradients, and therefore shifts in shoreline erosion and accretion patterns, than more uniform reef systems. **Citation:** Grady, A. E., M. A. Reidenbach, L. J. Moore, C. D. Storlazzi, and E. Elias (2013), The influence of sea level rise and changes in fringing reef morphology on gradients in alongshore sediment transport, *Geophys. Res. Lett.*, *40*, 3096–3101, doi:10.1002/grl.50577.

1. Introduction

[2] Climate-change-induced ocean warming and acidification, exacerbated by local-scale disturbances, are the primary threat to global coral reef health [e.g., *Anthony et al.*, 2011]. Frequent occurrences of mass coral bleaching and disease, combined with chronic secondary stressors such as eutrophication and overfishing, have set coral reefs on a trajectory toward ecosystem decline [e.g., *Pandolfi et al.*, 2003]. For many tropical coasts, reefs serve a critical function as primary breakwaters for incoming waves [e.g., *Ferrario et al.*, 2013]. As reef architecture is compromised through coral die-offs or shifts to algal dominance, wave energy dissipation may be reduced [*Sheppard et al.*, 2005]. Increasing coral mortality will result in decreased calcification and eventual erosion of reefal skeletons, which

has been shown to result in reef flattening [e.g., *Alvarez-Filip et al.*, 2009]. Compounding this issue is the potential for increased wave energy propagation as a result of higher relative sea level; *Church and White* [2011] quantified a significant acceleration in sea level rise (SLR) over the last century, potentially resulting in SLR of 0.5 m [*Intergovernmental Panel on Climate Change,*, 2007], or up to 1 m by 2100 [*Overpeck and Weiss*, 2009; *Nicholls and Cazenave*, 2010]. Shorelines exist in a dynamic equilibrium with local sea level and regional wave climate [e.g., *Slott et al.*, 2006]; variations in nearshore wave energy resulting from degrading reef architecture will affect this equilibrium. Changes to wave energy flux at the shoreline of reef-fronted beaches may lead to shifts in alongshore sediment transport gradients, thereby modifying the location and magnitude of shoreline erosion and accretion. Here, we investigate the potential influence of reef degradation and SLR on patterns of shoreline change in a fringing reef environment.

[3] We use a physics-based numerical model to simulate the response to changing conditions of two representative fringing reef morphologies (wide versus narrow reef flat). We assume that (a) coral reef skeletons will weaken due to decreasing reef calcification resulting from ocean acidification [e.g., *Kleypas et al.*, 1999] and subsequently that (b) erosion of coral reefs will be enhanced due to long-term physical, biological, and chemical processes acting on a degraded reef [e.g., *Rogers et al.*, 1982]. We combine potential SLR scenarios with our simulations of reef degradation to quantify the change in wave energy flux available to transport sediment along the reef-fronted coastline. We modeled hydrodynamic and alongshore sediment transport processes to explore how potential climate-change impacts on coral reef framework and sea level may alter nearshore wave energy flux on reefs, and ultimately modify the adjacent coastline.

2. Methods

[4] The fringing reef off the south shore of Molokai is the most extensive in the Hawaiian Islands, with variable morphologies along the entire reef tract. *Kench and Brander* [2006] established a statistically significant relationship between reef geomorphology and wave energy modification. The morphology of the Molokai reef, as well as meteorological and oceanographic conditions at the site, is representative of most exposed tropical fringing reefs [*Riegl and Dodge*, 2008], strengthening the transferability of our study to other reef sites.

[5] The objective here is not to produce precise estimates of shoreline change for Molokai beaches, but rather the schematized nature of the model domains and range of reef flat widths are intended to provide insights applicable to fringing reef environments worldwide.

[1]Department of Environmental Sciences, University of Virginia, Charlottesville, Virginia, USA.
[2]Department of Geological Sciences, University of North Carolina, Chapel Hill, North Carolina, USA.
[3]Coastal and Marine Geology, U.S. Geological Survey, Santa Cruz, California, USA.
[4]Deltares, Delft, Netherlands.

Corresponding author: A. E. Grady, Department of Environmental Sciences, University of Virginia, Clark Hall, 291 McCormick Road, Charlottesville, VA 22904, USA. (aeg4q@virginia.edu)
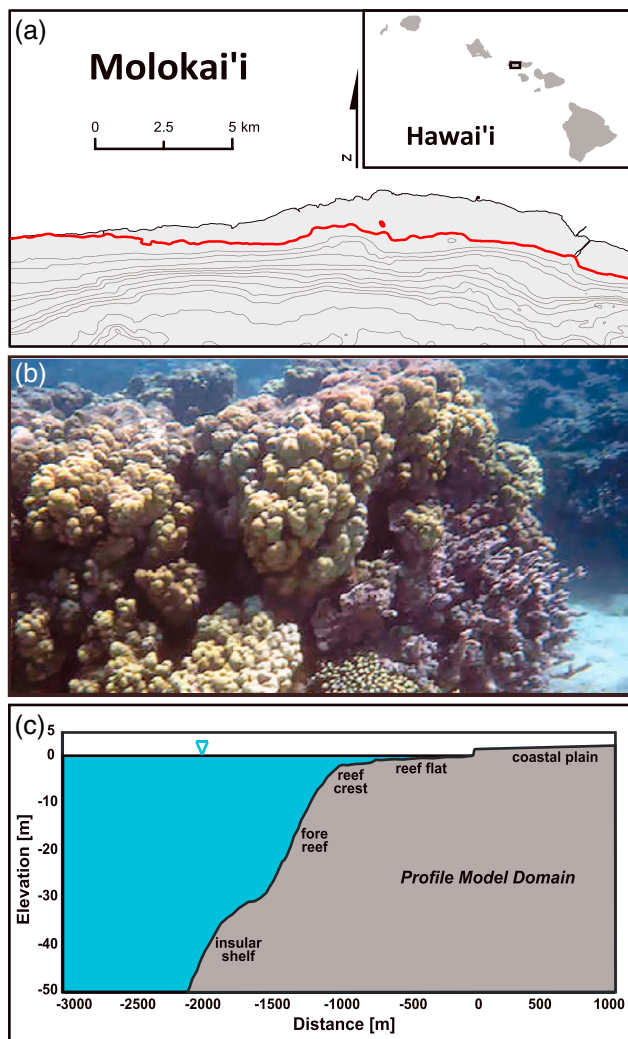
Figure 1. (a) Shoreline and nearshore bathymetric contours of the Molokai study area with inset of Hawaiian Islands. Bathymetric contour spacing is 10 m, with 50 m spacing at depths greater than 100 m. The approximate location of the reef crest is noted with the 2 m bathymetric contour line shown in red. (b) Underwater photo of coral located on the fore-reef. (c) Reef and nearshore bathymetry used in the profile model. Figure adapted from *Storlazzi et al.* [2011].

2.1. Study Area

[6] The island of Molokai is located in the Hawaiian archipelago between Oahu and Maui (Figure 1a). Four dominant meteorological forcings characterize the wave climate: northeasterly trade winds (significant wave height, H_s ~1–3 m, and dominant wave period, T_d ~5–8 s), southern swell (H_s ~1–2 m, T_d ~14–25 s), and during the winter, Kona storms and North Pacific swell (H_s ~3–6 m, T_d ~10–18) [*Moberly and Chamberlain*, 1964]. A 53 km-long fringing reef lies off the southern shore, partially sheltered from waves by neighboring islands. The Molokai reef is characterized by a shallow flat (0.3 to 2.0 m depth) that extends offshore up to 1.5 km (to the reef crest) [*Storlazzi et al.*, 2003]. The reefal hardground of the inner flat is covered in calcareous and finer terrigenous sediment, ridge-and-runnel structure characterizes the outer flat, and dominant wave breaking occurs on the crest,

covered by coralline algae and lobate encrusting corals. Seaward of the crest is the fore-reef (~3 to 30 m depth) with variable percentages of live coral cover on 1–3 m-high spur-and-groove structures (Figure 1b) [*Field et al.*, 2008].

2.2. Numerical Model

[7] We use the Delft3D modeling system [*Lesser et al.*, 2004] to simulate hydrodynamics over the Molokai reef. The Delft3D-FLOW module, which calculates currents by solving the unsteady shallow water equations, was coupled with stationary runs of the third-generation Simulating WAves Nearshore (SWAN) wave model, which solves the spectral action balance [*Booij et al.*, 1999]. We use the surfbeat/roller model extension to represent the effects of short-wave groups on long waves caused by spatial variations in radiation stresses [*Roelvink*, 1993]. The surfbeat/roller model accounts for long waves attaching to carrier short waves, which travel at the group velocity of the carrier waves. Wave breaking is the dominant process driving the flow and wave energy decay within the Molokai reef system [*Storlazzi et al.*, 2011]; wave breaking transforms wave energy into roller energy, which is propagated and dissipated through the roller energy balance in the surfbeat/roller model.

[8] Model hydrodynamics were calibrated and validated with high-resolution in situ field measurements of tides, waves, currents, and suspended-sediment concentrations [*Storlazzi et al.*, 2004]. Schematized tidal forcings following the *Lesser et al.* [2004] technique and sensitivity analyses contributed to the creation of seasonally schematized wind and wave forcings (Table S1); model construction and validation are described by *Storlazzi et al.* [2011].

[9] *Storlazzi et al.* [2011] used Scanning Hydrographic Operational Airborne Lidar Survey (SHOALS) lidar data [*Storlazzi et al.*, 2003] to construct a 10 m resolution, schematized, 2-D profile of the Molokai reef (Figure 1c), with geometry representing the wide shallow reef flat of the central reef system. To create a model domain representative of the western edge of Molokai, we created a new domain using the same calibrated atmospheric and oceanographic forcings as *Storlazzi et al.* [2011], in which reef flat width is reduced (by 10×) to 100 m.

2.3. Model Scenarios

[10] For each of the two model domains, we created bathymetric inputs to simulate incremental, physical breakdown of the fore-reef and reef crest. Because projected SLR rates are up to an order of magnitude greater than vertical accretion rates for exposed fringing reefs [e.g., *Buddemeier and Smith*, 1988], and the fringing reef at our study location has lost 80–90% of live coral coverage [*Field et al.*, 2008], we did not simulate the effect of changes in vertical accretion. We represent degradation by increasing the depth of the reef by 0.10, 0.25, 0.50, and 1.00 m in the zone of the most extensive coral growth (from ~30 to 2 m depth) for comparison with an unmodified base case simulation. We established a maximum coral breakdown value of 1.00 m, representing the lower bound of spur-and-groove heights on the Molokai fore-reef [*Storlazzi et al.*, 2003]. Following on the work of *Storlazzi et al.* [2011], we simulated the effect of elevated sea level (+0.10, +0.25, +0.50, and +1.00 m) for each model domain and reef degradation scenario, resulting in a suite of 50 simulations (+1.00 m SLR used in our model scenario is an order of magnitude greater than storm-induced setup or other local short-term variations in water level [*Fletcher et al.*, 2011]).
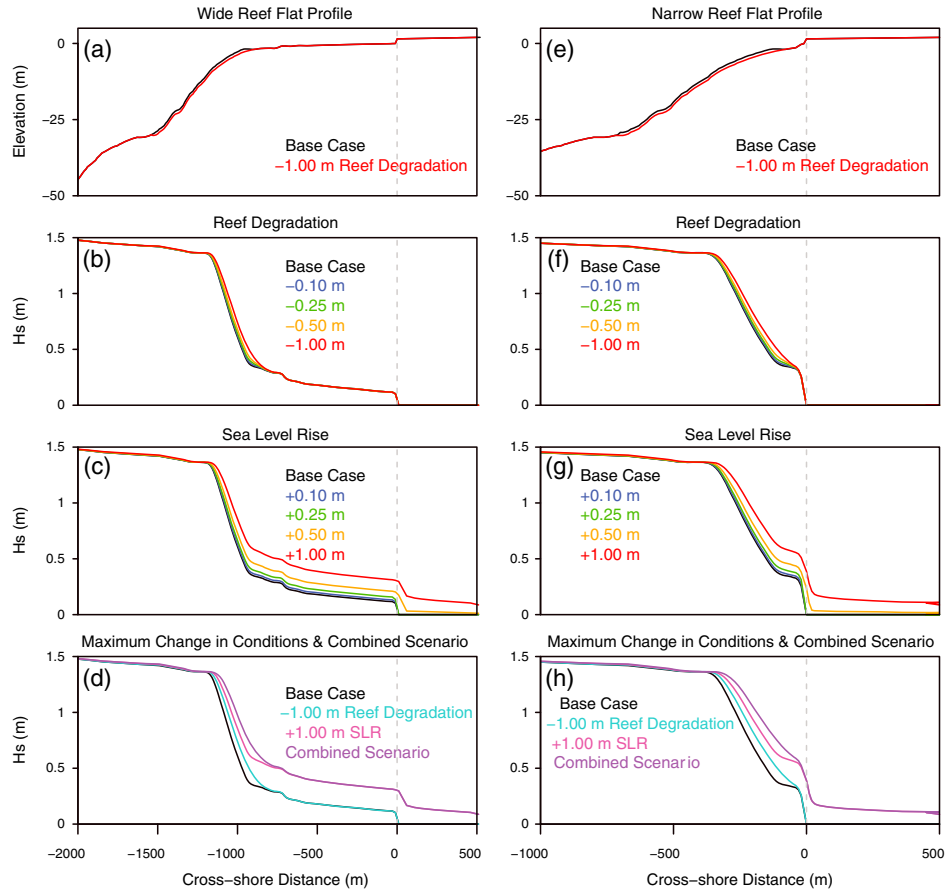
Figure 2. Modeled significant wave heights for a subset of wide and narrow reef flat scenarios. The dashed line represents shoreline position. (a and e) Original and degraded morphology of the model domain. (b and f) Reef degradation scenarios. (c and g) SLR scenarios. (d and h) Maximum variable conditions and maximum combined effect of reef degradation and SLR.

Model scenarios with the same magnitude of change (e.g., $+1.00$ m SLR, -1.00 m reef degradation) do not have the same outcome, as SLR changes the water level throughout the entire domain, while reef degradation generates a "pseudo-SLR" [*Sheppard et al.*, 2005] only within a restricted zone of the domain. The initial conditions for each simulation represent an instantaneous shift in reef state and/or sea level.

[11] We ran each simulation for one model year using annually-weighted environmental forcings. Storm conditions account for the greatest relative contribution to the annual sediment flux (63%), despite the low frequency of occurrence (~3% of the year, see Table S1) [*Storlazzi et al.*, 2011]; therefore, we isolated storm conditions, maintaining steady conditions, to calculate the relative influence of waves on alongshore sediment transport for different model scenarios. Alongshore sediment transport was calculated as [*Haas and Hanes*, 2004]

$$q_{HH} = \frac{2C_1}{\rho g} V_{my} \overline{|\tau|} \tag{1}$$

where C_1 is a tuning parameter determined from the *Coastal Engineering Research Center* [1984] formula, ρ is water density, g is gravity, V_{my} is depth-averaged alongshore current, τ is bottom shear stress, and the overbar represents time averaging over a short-wave period. In our calculations, we used a value of $C_1 = 1.3$ as determined by *Hass and Hanes*, [2004], and values of V_{my} and τ were calculated in

Delft3D model scenarios. We did not calibrate this constant for the Molokai site as our goal was to assess the change in sediment transport potential in each model scenario, rather than to reproduce or predict actual sediment transport. The contiguous nature of the Molokai reef crest causes wave-induced setup to occur in the alongshore direction, which results in alongshore currents that are nearly two to eight times greater than cross-shore currents. The shallow nature of the Molokai reef system and the absence of a significant reef channel network, along with wave-driven setup in the nearshore, cause flow and sediment transport in the alongshore direction to dominate [*Storlazzi et al.*, 2011], allowing us to focus on alongshore transport processes. We integrated the resulting potential alongshore transport rates over the duration of storm conditions and across the nearshore for each model scenario in the region extending from the shoreline to the reef crest. We compared the potential for storm-driven alongshore sediment transport across all simulations.

3. Results

3.1. Relative Influence of Coral Reef Degradation and SLR on Wave Height

[12] As coral degradation and sea level increased across simulations, the location of peak wave breaking moved shoreward as larger waves were able to propagate farther past the reef crest before undergoing depth-induced breaking
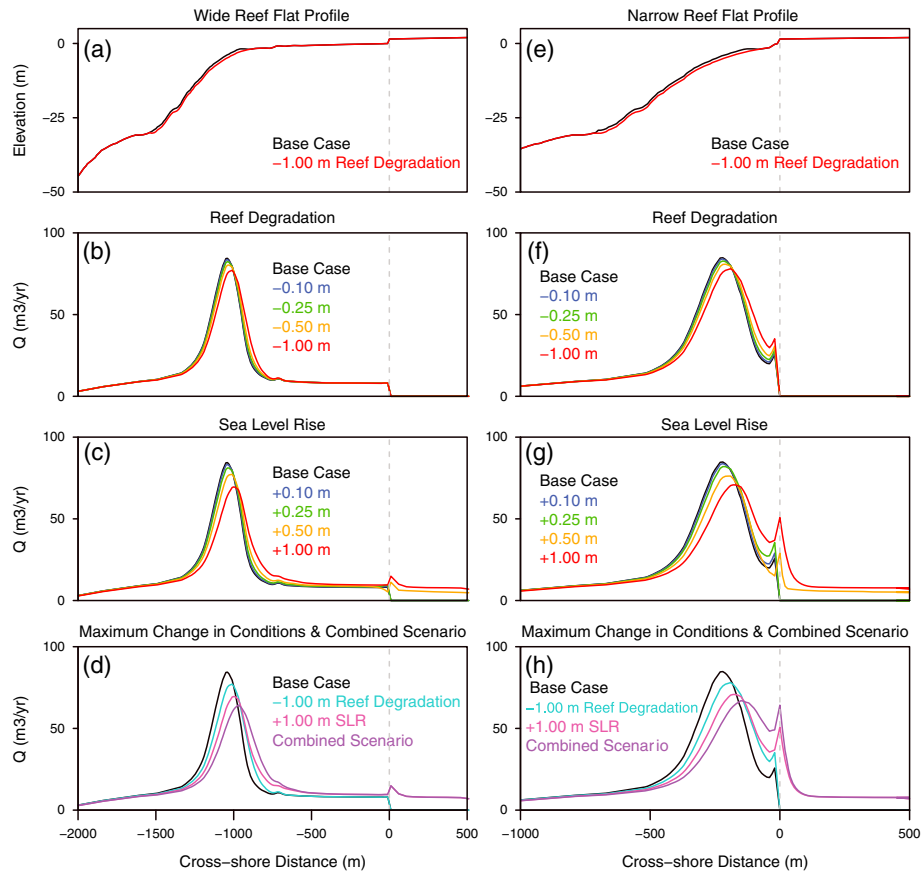
Figure 3. Potential volumetric alongshore sediment transport rates during storm conditions, for a subset of wide and narrow reef flat scenarios. The dashed line represents shoreline position. (a and e) Original and degraded morphology of the model domain. (b and f) Reef degradation scenarios. (c and g) SLR scenarios. (d and h) Maximum variable conditions and maximum combined effect of reef degradation and SLR.

(Figure 2). However, when simulating coral degradation across the wide flat, this change in wave heights was dampened by the shallow, depth-limited nature of wave transformation on the flat (Figure 2b). The addition of maximum reef degradation (1.00 m) to the maximum SLR (+1.00 m) scenario had little effect on wave height near the shoreline in the case of a wide flat (Figure 2d), but increased wave heights near the shoreline in the case of the narrow flat (Figure 2h). Nearshore wave heights nearly doubled (91.8% increase above the base scenario) over the narrow reef flat, with reef degradation providing one third of the percent increase (33.2% above the base scenario). For +0.50 m and +1.00 m SLR scenarios, storm conditions caused significant runup (>0.30 m) of waves onto the coastal plain in both model domains. The increased wave height in the nearshore is most evident over the shallow reef flat area and the newly inundated coastal plain (Figures 2c and 2g).

3.2. Potential Effects on Alongshore Sediment Transport

[13] SLR has a greater relative effect on alongshore sediment transport than reef degradation for the wide reef flat, with transport unaltered by degradation landward of the zone of wave breaking (Figures 3b and 3c). In contrast, reef degradation and SLR had a similar effect on alongshore sediment transport rate with a corresponding 62.6% and 82.8% increase above the base scenario in the narrow flat (Figures 3f and 3g). Further, over the wide flat, there was a detectable increase in alongshore sediment transport rate as a function of SLR, but degrading reef structure had a minimal effect. Although the zone of maximum transport was translated shoreward in all scenarios, only the narrow flat demonstrates a similar increase in potential alongshore sediment transport for both 1.00 m of reef degradation and +1.00 m of SLR.

Table 1. Potential Alongshore Sediment Transport Volumes During Storm Conditions Over One Model Year

Model Scenario	Wide Flat: Total Potential Alongshore Transport Volume (m^3/m)	Percent Change From the Base Scenario (%)	Narrow Flat: Total Potential Alongshore Transport Volume (m^3/m)	Percent Change From the Base Scenario (%)
Base Case	843.7	--	131.4	--
−1.00 m Reef Degradation	929.7	10.2	201.0	53.1
+1.00 m Sea Level Rise	1183.4	40.3	229.2	74.6
Maximum Combination	1325.4	57.1	421.7	134.8

[14] We integrated the potential alongshore sediment transport volume over the nearshore area, from reef crest to shoreline. In the case of the wide flat, the increase in potential transport volume for the maximum SLR scenario was nearly four times greater than the maximum reef degradation scenario (40.3% versus 10.2% above the base scenario), as shown in Table 1. However, with the narrow flat, the increase in transport for the maximum SLR scenario (74.6% above the base scenario) was approximately 1.5 times greater than for the maximum reef degradation scenario (53.1% above the base scenario). In a comparison between the two domains, maximum reef degradation increased transport for the narrow flat case by a factor of 5.2 above the wide flat, and a factor of 1.8 for maximum SLR. When the maximum values of the input variables were combined, transport in the narrow reef flat case was a factor of 2.4 greater than for the wide flat. Although sea level exerted more influence than reef degradation on changes in wave energy flux and potential alongshore sediment transport for the wide reef flat morphologies (Figures 2d and 3d), narrow reef flat environments were similarly responsive to changes in sea level and reef degradation (Figures 2h and 3h).

4. Discussion

[15] The purpose of this work was not to generate detailed predictions for any one site, but rather to investigate possible alterations to wave shoaling and sediment transport patterns across a reef in a schematized context, so that results apply to a range of locations. As such, the implications of this work must be considered in context of the following limitations. First, our model scenarios represent instantaneous shifts in physical reef state and sea level, when, in reality, such changes would be gradual, occurring across decades. Additionally, reef degradation would likely be heterogeneous, depending on the type and scale of disturbance, and coral resistance to stressors and physical breakdown. Our modeling approach does not account for the effects of gradual change or the heterogeneity of changes in the reef system, both of which may affect adjacent local beach response. The *Haas and Hanes* [2004] formulation is a simplified model of alongshore sediment transport, a product of bed shear stress that mobilizes sediment and alongshore current that transports it; although beach slope, grain size, and other site and sediment characteristics are not included, this level of parameterization is appropriate for conveying the relative difference between model domains. In addition, rates of sediment transport presented here would, in reality, be limited by nearshore sediment supply. Molokai beaches are most likely supply-limited; they are effectively isolated from the zone of major carbonate sand production, the fore-reef, by reef flat distance, and the shallow crest [*Calhoun and Field*, 2008]. However, we calculate sediment volumes under the assumption of a transport-limited system in order to provide insights that apply broadly to fringing reef ecosystems worldwide.

[16] Our results indicate that SLR appears to drive increases in alongshore sediment transport over wide reef flats through a reduction in the depth limitation for wave development, which, in turn, allows more wave energy to propagate toward shore. As a result, nearshore wave energy and alongshore sediment transport are both strongly influenced by rising sea level, with maximum values achieved in scenarios that simulate the combined effects of coral reef degradation and SLR. For the +0.50 m and +1.00 m SLR model scenarios, storm

waves produced significant runup onto the coastal plain. Model results indicated that SLR, not reef degradation, will cause greater reduction in attenuation of wave energy; however, enhanced coastal erosion would only occur if the increased wave energy flux results in changes in alongshore sediment transport gradients.

[17] The model results suggest that reef degradation will significantly increase wave height and alongshore sediment transport for narrow reef flats, but have little effect on areas with a wide flat. As a result of this disparity, the greatest difference in the rate of change in alongshore sediment transport between the two reef morphologies was due to reef degradation rather than SLR. The difference in the increase in alongshore sediment transport rates between the two domains suggests that shorelines protected by narrow reef flats would receive more wave energy for the same degree of reef degradation relative to shorelines protected by a wide flat. In the case of degraded fringing reef systems having alongshore-variable reef flat width, changes in alongshore sediment transport gradients may result, potentially driving changes in patterns of erosion and accretion at the shoreline. This indicates that the degree to which alongshore sediment transport gradients are altered will be a function of the nonuniformity in alongshore reef flat width. It is also evident that the addition of SLR to reef degradation reduces the difference in the increase in alongshore sediment transport rates between the two domains, indicating that degradation in the absence of SLR will likely result in the largest potential gradients.

[18] Although data do not exist to assess the percentage of reefs worldwide having alongshore-variable widths, aerial imagery suggests this is a common characteristic [*Hopley*, 2011]. Coral reef morphology and condition vary globally, but for fringing reef systems having alongshore-variable widths, our results indicate that coral reef degradation will likely result in more significant shifts in patterns of erosion and accretion than SLR of the same magnitude. Consequently, the most dramatic shoreline changes may occur in locations having alongshore-variable reef flat width in combination with rates of coral reef degradation that outpace SLR. These results demonstrate the existence of a previously unrecognized link between coral reef health and rates of shoreline change and imply that coordination of coral reef preservation and shoreline planning efforts may be a necessary component of integrated coastal zone management programs in tropical regions.

References

Alvarez-Filip, L., N. K. Dulvy, J. A. Gill, I. M. Côté, and A. R. Watkinson (2009), Flattening of Caribbean coral reefs: Region-wide declines in architectural complexity, *Proc. R. Soc. B*, *276*, 3019–3025, doi:10.1098/rspb.2009.0339.

Anthony, K. R. N., J. A. Maynard, G. Diaz-Pulido, P. J. Mumby, P. A. Marshall, L. Cao, and O. Hoegh-Guldberg (2011), Ocean acidification and warming will lower coral reef resilience, *Global Change Biol.*, *17*(5), 1798–1808, doi:10.1111/j.1365-2486.2010.02364.x.

Booij, N., R. C. Ris, and L. H. Holthuijsen (1999), A third-generation wave model for coastal regions: 1. Model description and validation, *J. Geophys. Res.*, *104*(C4), 7649–7666, doi:10.1029/98JC02622.

Buddemeier, R., and S. Smith (1988), Coral reef growth in an era of rapidly rising sea level: Predictions and suggestions for long-term research, *Coral Reefs*, *7*, 51–56.

Calhoun, R. S., and M. E. Field (2008), Sand composition and transport history on a fringing coral reef, Molokai, Hawaii, *J. Coastal Res.*, *245*, 1151–1160, doi:10.2112/06-0699.1.

Coastal Engineering Research Center (1984), Shore Protection Manual, U.S. Army Corps of Eng., Vicksburg, Miss.

Church, J. A., and N. J. White (2011), Sea-level rise from the late 19th to the early 21st century, *Surv. Geophys.*, *32*(4–5), 585–602, doi:10.1007/s10712-011-9119-1.

Ferrario, F. M., W. Beck, C. D. Storlazzi, F. Micheli, C. C. Shepard, and L. Airoldi (2013), Coral reefs are effective for coastal hazard risk reduction, *Proc. Natl. Acad. Sci. U.S.A.*, in press.

Field M. E., S. A. Cochran, J. B. Logan, and C. D. Storlazzi (2008), The coral reef of south Moloka`i, Hawai`i—Portrait of a sediment-threatened fringing reef, *U.S. Geol. Surv. Sci. Rep. 2007–5101*, Santa Cruz, Calif.

Fletcher, C. H., B. M. Romine, A. S. Genz, M. M. Barbee, M. Dyer, T. R. Anderson, S. C. Lim, S. Vitousek, C. Bochicchio, and B. M. Richmond (2011), National assessment of shoreline change: Historical shoreline changes in the Hawaiian islands, *U.S. Geol. Surv. Open File Rep. 2011–1051*, Santa Cruz, Calif.

Haas, K., and D. Hanes (2004), Process based modeling of total longshore sediment transport, *J. Coastal Res.*, *20*(3), 853–861.

Hopley, D. (2011), *Encyclopedia of Modern Coral Reefs: Structure, Form and Process*, Springer, Berlin.

Intergovernmental Panel on Climate Change (2007), *Climate Change 2007: The Physical Science Basis. Contribution of Working Group I to the Fourth Assessment Report of the Intergovernmental Panel on Climate Change*, edited by S. Solomon et al., pp. 747-846, Cambridge Univ. Press, Cambridge, U. K.

Kleypas, J. A., R. W. Buddemeier, D. Archer, J. P. Gattuso, C. Langdon, and B. N. Opdyke (1999), Geochemical consequences of increased atmospheric carbon dioxide on coral reefs, *Science*, *284*(5411), 118–120, doi:10.1126/science.284.5411.118.

Kench, P. S., and R. W. Brander (2006), Wave processes on coral reef flats: Implications for reef geomorphology using Australian case studies, *J. Coastal Res.*, *221*, 209–223, doi:10.2112/05A-0016.1.

Lesser, G. R., J. A. Roelvink, J. A. T. M. van Kester, and G. S. Stelling (2004), Development and validation of a three-dimensional morphological model, *Coastal Eng.*, *51*(8–9), 883–915, doi:10.1016/j.coastaleng.2004.07.014.

Moberly R. M., and T. Chamberlain (1964), Hawaiian beach systems, *Rep. HIG 64-2*, Hawaii Inst. of Geophys. Univ. of Hawaii, Honolulu, Hawaii.

Nicholls, R. J., and A. Cazenave (2010), Sea-level rise and its impact on coastal zones, *Science*, *328*(5985), 1517–20, doi:10.1126/science.1185782.

Overpeck, J. T., and J. L. Weiss (2009), Projections of future sea level becoming more dire, *Proc. Natl. Acad. Sci. U. S. A.*, *106*(51), 21,461–21,462, doi:10.1073/pnas.0912878107.

Pandolfi, J. M., et al. (2003), Global trajectories of the long-term decline of coral reef ecosystems, *Science*, *301*(5635), 955–8, doi:10.1126/science.1085706.

Riegl, B. M., and R. E. Dodge (2008), *Coral Reefs of the USA*, Springer, Syracuse, N.Y.

Roelvink, J. A. (1993), Dissipation in random wave groups incident on a beach, *Coastal. Eng.*, *19*, 127–150.

Rogers, C. S., T. H. Suchanek, and F. A. Pecora (1982), Effects of hurricanes David and Frederic (1979) on shallow *Acropora palmata* reef communities: St. Croix, US Virgin Islands, *Bull. Mar. Sci.*, *32*(2), 532–548.

Sheppard, C., D. Dixon, M. Gourlay, A. Sheppard, and R. Payet (2005), Coral mortality increases wave energy reaching shores protected by reef flats: Examples from the Seychelles, *Estuarine Coastal. Shelf Sci.*, *64*(2–3), 223–234, doi:10.1016/j.ecss.2005.02.016.

Slott, J. M., A. B. Murray, A. D. Ashton, and T. J. Crowley (2006), Coastline responses to changing storm patterns, *Geophys. Res. Lett.*, *33*, L18404, doi:10.1029/2006GL027445.

Storlazzi, C. D., J. B. Logan, and M. E. Field (2003), Quantitative morphology of a fringing reef tract from high-resolution laser bathymetry: Southern Molokai, Hawaii, *Geol. Soc. Am. Bull.*, *115*(11), 1344–1355, doi:10.1130/B25200.1.

Storlazzi, C. D., A. Ogston, M. Bothner, M. Field, and M. Presto (2004), Wave- and tidally-driven flow and sediment flux across a fringing coral reef: Southern Molokai, Hawaii, *Cont. Shelf Res.*, *24*(12), 1397–1419, doi:10.1016/j.csr.2004.02.010.

Storlazzi, C. D., E. Elias, M. E. Field, and M. K. Presto (2011), Numerical modeling of the impact of sea-level rise on fringing coral reef hydrodynamics and sediment transport, *Coral Reefs*, *30*(S1), 1–14, doi:10.1007/s00338-011-0723-9.